SHEDDING LIGHT ON THE PHOTOREPAIR OF ULTRAVIOLET RADIATION INDUCED DNA DAMAGE IN GOLDFISH (*CARASSIUS AURATUS*) EMBRYOS

BARBARA M. GAJDA

SUPERVISED BY: DAWN. A. H. RITTBERG
COMMITTEE: DRS. ALBERTO CIVETTA AND DONNA YOUNG

A THESIS SUBMITTED IN PARTIAL FULFILLMENT OF THE HONOURS THESIS COURSE (05.4111/6)

DEPARTMENT OF BIOLOGY
UNIVERSITY OF WINNIPEG
2003

ABSTRACT

Cyclobutane pyrimidine dimers (CPDs) are DNA lesions caused by the absorption of ultraviolet radiation (UVR) by nucleic acids. Photorepair is an important protective mechanism in organisms exposed to ultraviolet radiation and involves the enzyme photolyase that uses a photon of light to monomerize CPDs. This research investigates photorepair ability in goldfish embryos by correlating changes in mortality and morbidity under various UVR treatments with the presence of CPDs. Goldfish embryos were exposed to UV irradiation with and without phototherapy according to four treatment regimes. After hatching, the frequency of dead or morphologically abnormal larvae was compared between treatment groups. An endonuclease sensitive site (ESS) assay was performed on DNA extracted from embryos. The ESS assay uses T4 endonuclease V that produces a single stranded nick in DNA at the site of CPDs. A decrease in the molecular weight of T4 endonuclease treated DNA correlates to an increased frequency of CPDs. The absence of visible light prior to and following irradiation induced vulnerability in the embryos resulting in anatomical abnormalities or death. CPD frequencies are highest in the irradiated groups that received no phototherapy. Photorepair experiments and ESS assay results suggest that the production of CPDs during UVR exposure is a factor in the increased mortality of embryos that do not receive phototherapy.

ACKNOWLEDGEMENTS

I have been blessed with many wise and wonderful people in my education career and life who have guided me with their insight and knowledge. Dawn Rittberg has been a wonderful supervisor whose guidance and advice were invaluable. Dawn always knew exactly when I needed a little push or needed a little extra time during my hectic course schedule. I would also like to recognize my committee members Drs. Civetta and Young. The access I was granted to the Gel Doc 2000 camera by Dr. Civetta was vital to the completion of my research.

Thanks, Dr. Wiegand, for the summer evenings and weekends of sorting through fish and counting eggs. Thank you for your generosity of your experience with statistics and, mostly, for taking an active interest in the success of my research.

The expertise of Jeff Babb was invaluable in the statistical design and aftermath of the experiment. I appreciate the time and knowledge that he shared. I am grateful to Dr. Heubner and Nancy Loadman, for welcoming me to the UV lab and to Dr. Moodie, for his guidance in the thesis course. The technical staff of the Biology department, specifically, Susan Wiste, Terry Durham, Geri Damiani, Linda Buchanan and Tara Powell, have be integral to the completion of my work. Liza, Danielle, Nicole, Kent and Talia (Sun Savvy Team 2002) were essential for getting me started off onto the right foot.

Most importantly, I must credit my family who has indoctrinated into me the importance of hard work, optimism and taking one day a time. Your patience, love and strength have been unconditional and unparalleled.

TABLE OF CONTENTS

ABSTRACT I

ACKNOWLEDGEMENTS II

TABLE OF CONTENTS III

LIST OF TABLES IV

LIST OF FIGURES V

LIST OF APPENDICES VI

INTRODUCTION 1

MATERIAL AND METHODS 11

FERTILIZATION 11

IRRADIATION CHAMBER AND UV INTENSITIES 12

PHOTOREPAIR EXPERIMENTS

ILLUMINATED TRIALS 13

NON-ILLUMINATED TRIALS 17

DATA ANALYSIS 17

DNA DAMAGE ANALYSIS

CALF THYMUS DNA TRIALS 19

GENOMIC GOLDFISH DNA TRIALS 22

DATA ANALYSIS 23

RESULTS 24

EMBRYO SURVIVAL DATA 24

CALF THYMUS ESS ASSAY 27

GOLDFISH ESS ASSAY 27

DISCUSSION 35

CONCLUSIONS 40

REFERENCES 41

APPENDICES 45

LIST OF TABLES

Table I: PAR and UVR schedule for each of the treatment groups during the pre-illuminated photorepair experiments. 16

Table II: PAR and UVR schedule for each of the treatment groups during the photorepair experiments without pre-illumination. 18

Table III: Digestion protocol for calf thymus DNA. 21

Table IV: Results of Tukey's HSD test showing pairwise comparisons of goldfish embryo survival between treatment groups in non-illuminated photorepair experiments. 26

Table V: Randomized block model ANOVA and Tukey's HSD multiple comparison tests results for goldfish endonuclease sensitive site assay. 31

LIST OF FIGURES

Figure 1: Layout inside the irradiation chamber. 14

Figure 2: The effectiveness of treatment in illuminated and non-illuminated photorepair experiments on the arcsine square root transformed percentage of anatomically normal larvae (± standard error). 25

Figure 3: Profile of fluorescence intensity distribution over the migration distance of calf thymus DNA. 28

Figure 4: Densitometric scan of the distribution of fluorescence in relationship to migration distance for goldfish gel 3. 30

Figure 5: Average molecular length of goldfish DNA samples digested with T4 endonuclease V and electrophoresed under alkaline conditions. 33

Figure 6: The frequency of endonuclease sensitive sites (ESS) per base in goldfish DNA samples, grouped by gel number, that have been digested by T4 endonuclease V. 34

LIST OF APPENDICES

Appendix A: Artificial Insemination Medium (AIM) 42

Appendix B: Calf thymus DNA trials for testing protocol for detection of cyclobutane pyrimidine dimers using endonuclease sensitive site (ESS) assay. 43

Appendix C: Phenol-chloroform extraction of DNA from goldfish embryos. 44

Appendix D: Goldfish DNA trials: Protocol for detection of cyclobutane pyrimidine dimers using endonuclease sensitive site (ESS) assay. 45

INTRODUCTION

Radiation emitted from the sun includes a broad range of wavelengths. Outside Earth's atmosphere, 51% of the radiation is in the infrared (IR; >700 nm) spectrum, 41% is photosynthetically active radiation (PAR; 400 – 700 nm) and 8% comprises the three types of ultraviolet radiation (UVR; UV-A 320 – 400 nm; UV-B 280 – 320 nm; UV-C 200 – 280 nm) (Whitehead *et al.* 2000). The ozone layer will absorb UVR wavelengths less than 320 nm, however with disintegration of the ozone through interactions with anthropogenic compounds *(*Whitehead *et al.* 2000*),* wavelengths of 290 nm and longer are reaching Earth's surface (Setlow 2002). Inside the atmosphere, IR and PAR each makeup 45 – 50% and UVR comprises 1 – 5% of the radiation to which organisms are exposed. Overall, the diminishing thickness of the ozone layer leads to a shift towards shorter wavelengths and increases the total intensity of radiation reaching the surface of the Earth (Whitehead et al. 2000).

The toxic effects of UV exposure are initiated in two ways in the cell. Directly, proteins and nucleic acids with UVR and light absorbing groups, or chromophores, will absorb the UVR, causing degradation or transformation of the molecules and possibly arresting the biological function of the molecule (Vincent and Neale 2000). Indirect mechanisms include the production of reactive oxygen species (ROS) such as hydrogen peroxide, superoxides and hydroxyl radicals by photosensitizers. Upon absorbance of UVR, the electrons of photosensitizing molecules are excited to higher energy levels. The decomposition from the higher energy state to a lower energy state releases energy, which is transferred to oxygen producing ROS. ROS participate in fast reactions and diffuse in the cytosol, causing damage to macromolecules (Vincent and Neale 2000).

Nucleic acids have high absorbance coefficients for short UV wavelengths, peaking at 260 nm (UV-C), but extending into the UV-B range. When a pyrimidine or purine group absorbs a photon of UVR, the energy from absorption results in an excited singlet state, which exists for approximately a picosecond. The energy from the excited singlet either dissipates thermally or is used in chemical reactions, such as the photodestruction of nucleotides (Vincent and Neale 2000). Three photoproducts that result from UVR absorption are cyclobutane pyrimidine dimers (CPDs), photohydrates and (6-4) photoproducts (Vincent and Neale 2000).

CPDs, or 5,6-dipyrimidines, form between adjacent pyrimidines on a DNA strand in a *cis-syn* conformation (Vincent and Neale 2000) and are attributed responsibility for the majority of cell killing (Shima and Setlow 1984). Dimers located on the template strand during replication or transcription will inhibit DNA or RNA polymerases (Setlow 2002). The persistent presence of CPDs results in the development of preapoptotic and apoptotic features (Nishigaki *et al.* 1998). Immediate apoptosis, which can be prevented by vitamin E, is induced by damage to cellular membranes; whereas, delayed apoptosis is induced by DNA damage. In the context of UVR exposure, mostly CPDs and some other lesions will trigger delayed UV-induced apoptosis (Nishigaki *et al.* 1998).

Photohydrates are produced by the photoaddition of water across the 5,6-ethylenic bond in pyrimidine bases. Although the quantum yield (number of molecules inactivated per photon absorbed) of photohydrates is comparable to CPDs, these lesions degrade within hours and therefore have no detectable biological effect (Vincent and Neale 2000). Although pyrimidine (6-4) pyrimidones, or (6-4) photoproducts ((6-4)PP) are produced at a tenth of the frequency as CPDs, these photoproducts are more effective than CPDs at

blocking transcription by DNA polymerase (Vincent and Neale 2000). Interestingly, these lesions are repaired more efficiently by nucleotide excision repair than CPDs (Koehler et al. 1996). After its formation, the (6-4)PP can be converted into the more lethal, less mutagenic Dewar pyrimidone (Mitchell and Nairn 1989).

Protein damage also occurs as a result of UVR absorbance by the functional groups of the aromatic amino acids. The aromatic groups act as photosensitizers and the resulting ROS diffuse in the cytoplasm, oxidizing amino acid residues of other proteins and causing degradation or cross-linking (Vincent and Neale 2000).

Four responses to UVR stress have evolved in aquatic organisms: avoidance, screening, acclimation and repair. Avoidance most relevantly applies to organisms with photosensors that can detect radiation in the UV range. These organisms will migrate from the light, moving either deeper into the water column or into shaded areas, or will inhabit areas without direct light (Roy 2000). Extracellular screenings, such as melanin, are found and produced in the skin of aquatic vertebrates. Intracellular screenings often cannot be produced but must be accumulated through diet or symbiotic relationships. Fish are known to accumulate mycosporine-like amino acids (MAA), which function as sunscreen (Roy 2000). Acclimation often takes the form of permanent accumulations of MAAs and antioxidants (Roy 2000).

Repair takes many forms depending on the type of damage. Antioxidant enzymes and molecules, such as carotenoids, will reduce and inactivate ROS. Protein repair involves the production of heat shock proteins where transcription and translation is induced by accumulation of damaged proteins. Heat shock proteins solubilize denatured proteins for either degradation or salvaging by restoration to their native form through refolding (Roy

2000). Nucleic acid repair is accomplished through nucleotide excision repair (NER) and photoenzymatic repair, or photoreactivation (PR).

Highly conserved in eukaryotes, NER removes a wide range of DNA lesions. Two subpathways of NER exist. Transcription-coupled repair (TC-NER) preferentially repairs actively transcribed genes in 'gene-specific repair' and repairs transcribed strands faster than non-transcribed strand in 'strand-specific repair'. Global genome repair (GG-NER) non-specifically repairs lesions in the entire genome, including non-transcribed segments (Thoma 1999). NER is a multistep process, involving first the recognition and binding of damaged DNA by damage detecting proteins. General transcription factors are recruited to form an open complex followed by DNA helicases that unwind the DNA. Recruited nucleases make incisions directly 3′ and 5′ of the lesion and the resulting gap is filled by DNA synthesis and ligation (Thoma 1999). Because of the complexity of the NER system, NER is limited by the accessibility of the damage in chromatin. Therefore actively transcribed genes that are more accessible are preferentially repaired by NER. In contrast, photoreactivation is a simple repair mechanism and repairs damage in the entire genome non-preferentially (Komura *et al.* 1991).

The enzyme responsible for the photoreactivation of CPDs, photolyase, is found in many organisms, ranging from prokaryotes to marsupials (Yasui *et al.* 1994). Photolyase is a single peptide enzyme of 55-66 kDa (Aubert *et al.* 2000). Two classes of photolyase exist. In both classes, the presence of FAD as a catalytic chromophore in the active site is intrinsic to enzyme composition. Class I, also referred to as microbial photolyases, is comprised of two highly homologous types of photolyase, distinguished by the chromophores present. FAD is the primary chromophore for all photolyases; however, class I photolyases contain

a secondary chromophore, either methenyltetrahydrofolate (MTHF) or 8-hydroxy-5-deazaflavin (8-HDF), to harvest photons for catalysis. Class I photolyases are found primarily in prokaryotes, however some plant photolyases have been shown to be highly homologous (Yasui *et al.* 1994). Only a 10-17% sequence homology exists between class I and II photolyases (Yasui *et al.* 1994) compared to the 25 – 80% homology within each class (Todo 1999).

Class II photolyases are found mostly in higher eukaryotes and some methanobacteria and eubacteria. These photolyases only contain FAD, which alone is sufficient for enzymatic activity (Yasui *et al.* 1994). Although no placental mammal homologue for photolyase has yet been discovered, other damage recognition roles for photolyase have been suggested (Ozer *et al.* 1995; Fox *et al.* 1994). Photolyase activity in vertebrates is often found to be higher in organs that have little or no potential for UV-induced damage, such as in chicken and opossum brain (Ozer *et al.* 1995). Therefore, it is speculated that in placental mammals, the function of photolyase has diverged from CPD-splitting to a degree that the sequence and function are not similar to known photolyases (Yasui *et al.* 1994). In *Escherichia coli*, photolyase has been observed to stimulate (A)BC exonuclease, an NER enzyme (Ozer *et al.* 1995). Contrary to its action in *E. coli*, photolyase in yeast (*Saccharomyces cerevisiae*) inhibits NER by binding and blocking the recognition of chemically induced DNA damage (Fox *et al.* 1994).

In addition to the photolyase which repairs CPDs, (6-4)PPs can be photoreactivated by another photolyase that has been identified in *Drosophila* (Todo *et al.* 1994) and goldfish (Uchida *et al.* 1997), (6-4) photolyase. Presently, the general molecular characteristics of (6-4) photolyase are presumed to be similar to those characteristics common to all CPD

photolyases (Todo 1999). However, the activity of CPD photolyase is higher in cultured goldfish cells than (6-4) photolyase (Uchida *et al.* 1997). (6-4) photolyase conserves a fully reduced form of FAD in the active form of the enzyme resulting in high sequence similarity to CPD photolyases. The reaction mechanism is different because the reaction cannot be simply a reversal of the formation. (6-4)PPs production involve a hydroxy (or amino group) transfer from C-4 on the 3´ base to C-5 on the 5´ base concomitant with the sigma bond formation between C-6 of the 5´ base and C-4 of the 3´ base (Todo 1999).

The ability of (CPD) photolyase to ameliorate the effects of UV-induced damage in DNA rests on the specific binding of the CPD. The mechanism of binding is sequence independent and the enzyme can bind to DNA that is superhelical, open circular or linear (Medvedev and Stuchebrukhov 2001). DNase I footprinting assays (Husain *et al.* 1987) determined that photolyase binds with close contact to the phosphate backbone including the first phosphodiester bond 5´ to the dimer and the third phosphodiester bond 3´ to the dimer. In fact, the minimum requirement for binding is the dimer itself; however, the additional sites function to increase binding affinity (Husain *et al.* 1987). Upon binding, the dimer conformation is altered to a flipped out conformation (Medvedev and Stuchebrukhov 2001), which induces conformational changes in the complementary strand. These changes are a result of enzyme binding and are not necessary for initial binding (Husain *et al.* 1987). The active site of the enzyme is concave, positively charged with the isoalloxazine ring of the flavin at the base of the hole (Komori *et al.* 2001). In class I photolyases, whose reaction mechanism has been studied in more detail than class II, the FAD cofactor is located deep in a cavity in a U-shape conformation to provide a docking site for the CPD (Carell *et al.* 2001; Medvedev and Stuchebrukhov 2001). The secondary cofactor is located in a shallow groove on the surface of the enzyme in order to absorb light

energy (Carell *et al.* 2001). The absorption of a photon by the MTHF or HDF group starts an intraprotein radical transfer cascade until the flavin is fully reduced from FADH to $FADH^{-}$ (Carell *et al.* 2001). The tryptophan-306 group is oxidized by the excited $FADH^{\bullet}$ and then reduced by the secondary chromophore or exogenous electron donors (Aubert *et al.* 2000). The transfer of energy from the chromophore to the flavin follows Förster's mechanism where the rate of transfer depends on distance. Distances between the cofactors in photolyase are kept relatively long, at some cost to rate, to prevent short-circuiting. The reduction potential for the second chromophore is often more positive than the dimer reduction potential which can result in the electron flow returning to the MTHF or HDF (Carell *et al.* 2001). Class II photolyases lack light harvesting chromophores; therefore, the electrons on the flavin must be excited by photon absorption by tryptophan residues or the direct absorption of light energy by the flavin (Medvedev and Stuchebrukhov 2001).

When the electron flow reaches and fully reduces the flavin cofactor, the key element of the reaction is the transfer of the electron from the flavin to the dimer (Medvedev and Stuchebrukhov 2001). The electron transfer causes a rearrangement of the electrons in the dimer and breaks the bonds holding the dimer. The electron is transferred indirectly through an intermediate through the adenine moiety. The configuration of the isoalloxazine ring brings the flavin and adenine close enough that electron density moves from the flavin to the adenine. The electron density flows according to conservation of quantum probability where a decrease in probability on one atom results in an increase in probability in a neighbouring atom (Medvedev and Stuchebrukhov 2001). When the current is localized on the adenine, the electron flow equilibrates as a circular current moving within the aromatic rings. The oxygen atoms in the thymine rings are the electron acceptors from the adenine (Medvedev and Stuchebrukhov 2001).

Yeast has been the model organism for studying the induction of photolyase. Several factors have been implicated in the regulation of gene expression of *PHR1*, the photolyase structure gene. The photolyase regulatory protein (PRP) is a transcriptional repressor of photolyase, which binds to an upstream repressor sequence (URS_{PHR1}). In undamaged yeast cells, PRP remains bound to the URS_{PHR1}; however, upon UV irradiation, the PRP dissociates from the regulatory site and *PHR1* expression increases (Sebastian and Sancar 1991). In addition to PRP, a positive regulator of *PHR1* transcription, *UME6*, enhances the basal-level expression of photolyase during general stress through interaction with an upstream activator sequence (UAS_{PHR1}) (Sweet *et al.* 1997). Despite the cross talk between the multistress response and the DNA damage response pathways in yeast (Jang *et al.* 1999), *PHR1* is not induced by heat shock and the response of *PHR1* to UV exposure is different than the general stress response (Sweet *et al.* 1997).

Specifically in cultured goldfish cells, photolyase expression is induced by visible (fluorescent) light and ROS production by photosensitizers. Neither the application of DNA damaging chemical agents and exogenous photolyase nor heat shock induces an increase in photolyase activity or transcription in the RBCF-1 cell line, derived from the goldfish caudal fin (Mitani and Shima 1995). In contrast, the level of *phr* expression in RBCF-1 cell cultures increases 10-fold upon exposure to visible light (Yasuhira and Yasui 1992). Preillumination with visible light prior to UVR exposure will increase cell survival and CPD removal since activation by visible light converts photolyase from its inactive to active form (Yasuhira *et al.* 1991). Mitani *et al.* (1996) suggest that *phr* expression in RBCF-1 cells is induced by the oxygen species produced by photosensitizers upon exposure to UV-A and fluorescent light, particularly blue wavelengths.

Unfortunately, the majority of research on photoreactivation of UV induced DNA damage in goldfish has been studied using the RBCF-1 cell line and not entire organisms. In organisms, the net damage is a function of competing damage and repair processes. The relationship between dose rate and dimer formation will change due to the higher number of cell layers which attenuate UVR (Vetter *et al.* 1999). The outermost layers of epithelial cells will absorb most of the harmful wavelengths of UVR before it reaches deeper cells such as melanophores. Consequently, pigmentation due to melanophores will have little effect on UV absorption (Funayama *et al.* 1994). Studies on North Sea plaice (*Pleuronectes platessa*) embryos (Dethlefsen *et al.* 2001) reveal that carotenoids and cuticular melanin, used by planktonic organisms as a means of UVR protection, are absent in young fish embryos (Dethlefsen *et al.* 2001). Even the egg chorion provides no protection from the penetration of UVR (Vetter *et al.* 1999). In plaice, the effects of UVR include impaired respiratory control in larvae and loss of positive buoyancy leading to increased mortality in embryos (Steeger *et al.* 2001). The mortality of embryos is dose dependent and developmental stage dependent (Dethlefsen *et al.* 2001).

Studies on medaka (*Oryzias latipes*) indicate that fish cells have higher photoreactivation ability than dark repair ability for CPDs (Nishigaki *et al.* 1998). Also, Northern anchovy (*Engraulis mordax*) embryos have a robust constitutive photorepair system by 6 hours post-fertilization (Vetter *et al.* 1999). Fifty-nine percent of UV-induced killing in fish embryos is attributed to CPDs (Applegate and Ley 1988). The dimers are effective transcription blocking lesions; therefore, rapid dimer removal from the genome by photoreactivation can significantly increase survival (Komura *et al.* 1991).

Therefore, the objectives of this research were to establish if goldfish embryos are capable of photorepair at the organismal level and to determine if a correlation exists between the persistence of CPDs and changes in embryo survival.

Materials and Methods

Fertilization

Fertilization protocol follows methods described in Wiegand *et al.* (1989). Fish purchased from Ozark Fisheries, Stoutland, MO, U. S. A., in March 2002 were held at 12-15°C under a photoperiod of 14L: 10D to simulate Winnipeg spring photoperiod. To initiate the fertilization procedure, females with vitellogenic eggs were removed from the stock tank into a separate warming tank overnight. In the morning, after the temperature had reached 20 - 22°C, the female fish were transferred to the spawning tank. Male goldfish producing milt were removed from the stock tank and allowed to warm to room temperature in the warming tank during the day and were transferred into the spawning tank in the evening. A mesh screen divided the spawning tank to allow the diffusion of female pheromones to the entire tank. Floating plants were also placed in the section containing the females to encourage ovulation. Ovulation was induced in the August set of fertilizations by administering pimozide (10 µg/g) and des-Gly^{10}-[D-Ala^{6}]-LHRH ethylamide (0.1 µg/g) (Wiegand *et al.* 1989).

On the spawning day, males were anaesthetized in a solution of ethyl *m*-amino benzoate (0.1-0.4% w/v). Milt was collected from each male by gently squeezing the abdomen from anterior to posterior. The fish and container were both kept dry and on ice to prevent the premature activation of the sperm. Once milt from all the males had been collected and vortexed gently, each female was anaesthetized individually and blotted dry. Eggs were expressed, by squeezing the abdomen anterior-posteriorly, into small petri dishes (4 cm diameter; Phoenix Biomedical) containing 10 mL Tris-buffered artificial insemination medium (AIM) (Appendix A). The AIM was buffered to pH 9.1 in order to counteract the

decrease in pH, which occurs during the increase in carbohydrate metabolism immediately after fertilization. Milt (11 µL) was immediately added to the dishes and swirled for uniform distribution. Clumps of eggs were separated with a stream of AIM from a Pasteur pipette. After incubating for 15 minutes at 22°C, the AIM from the dishes was decanted. The dishes were rinsed two or three times with AIM and then filled with 4-5 mL of dechlorinated water for further incubation. The total number of eggs in the dishes was 68 ± 32 (SD). The dishes were randomly distributed between the treatment groups with equal representation of each fish in each treatment group.

Dead embryos were removed 6 hours post-fertilization. Fertilization rate was determined as the percentage of embryos alive at 6 hours post-fertilization out of total eggs. Except during dark incubation periods, dead embryos were counted and removed daily. As well, the dishes were refreshed with aerated dechlorinated water. After hatching, larvae were individually counted and categorized as dead, anatomically abnormal or normal. Anatomical abnormalities include enlarged pericardial sacs, spinal deformations and/or abnormal development of the head (Wiegand *et al* 1989).

Irradiation chamber and UV intensities

Constructed of wood, the irradiation chamber measured 65 cm high, 140 cm wide and 70 cm deep with the interior painted white to increase reflection. The front of the chamber was left open to encourage air circulation and prevent excessive temperature increases caused by heat emanating from the bulbs. UVR and PAR were administered from one UV-B bulb (Philips TL40W/12 RS), four UV-A bulbs (Philips F40BLB 40W T12) and four high output cool white fluorescent bulbs (Philips F48T12CWHO).

The fluence rate of UV-B ($\mu W/cm^2$), UV-A (W/m^2) and PAR (W/m^2) were measured using the PMA2100 light meter/datalogger with detectors for PAR (PMA2132), UV-B (PMA2102) and UV-A (PMA2111) (Solar Light Co., Philadelphia). Light intensity within the chambers varied along the length of the bulbs as well as from the front to the back of the chamber. To remedy the intensity differences, the plates were randomly moved daily.

The high output of the bulbs tended to increase the temperature in the dishes above the range of 20-22ºC. To counteract the heat from the bulbs, the dishes were placed in water baths held at 22ºC. Three rectangular (85 cm length x 15 cm deep x 40 cm wide) Rubbermaid™ storage containers were placed lengthwise in the chambers (Figure 1). The petri dishes containing the embryos were placed randomly on 30 x 30 cm grids and fastened with transparent, non-fluorescing nylon thread. The grids were raised to 8 cm above the bottom of the Rubbermaid™ tub, a level not shaded by the sides of the tub. The tubs were filled until water reached approximately halfway up the side of the petri dishes. Air stones attached to small air pumps were placed in the water baths for water circulation. The amount and circulation of the water was effective in maintaining the water temperature in the plates below 23ºC.

Photorepair experiments

Illuminated trials

To determine if phototherapy reduces the damaging effects of UV-B irradiation, the embryos were exposed to UV-B radiation on day 3, approximately 48 hours post-fertilization. As previously determined in time course experiments (Thuen 2002), irradiation

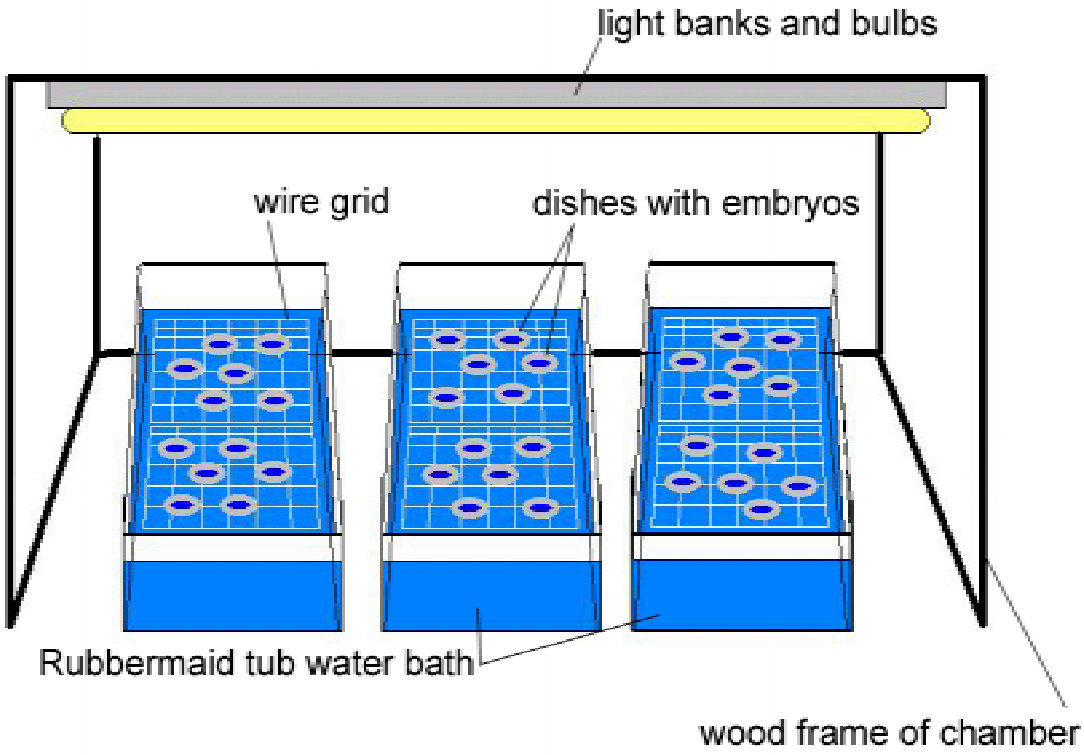

Figure 1: Layout inside the irradiation chamber. Petri dishes were placed upon wire grids in large waterbaths used to maintain temperature of the dishes between 20 – 22°C. Air stones (missing from diagram) were used to circulate water around the dishes.

with UV-B on day 3 resulted in no significant damaging effects. Four treatment groups were designed to both irradiate the embryos and determine the effect of incubating the embryos in darkness post-irradiation (Table I). All the groups, light control (LC), light experimental (LE), dark control (DC) and dark experimental (DE), were incubated with a 14L:10D photoperiod with PAR and UV-A until irradiation at approximately 48 hours post-fertilization. Over 14 hours, PAR and UV-A fluence rates were approximately 16 W/m^2 and 6 W/m^2, respectively, giving doses of 806.4 kJ/m^2 and 302.4 kJ/m^2, respectively. The experimental groups were irradiated between 09:00 and 13:00 at about 48 hours post-fertilization. The dose of UV-B radiation administered to the embryos was approximately 2.16 kJ/m^2. Control groups were shielded from exposure to UV-B radiation with Mylar® polyester film (type D, 0.003 inch thickness, Cadillac Plastics, Winnipeg). After the period of irradiation, the dark groups were placed in another Rubbermaid™ tub water bath, outside the chamber, and covered in black plastic (medium duty polyethylene, Canadian Tire) such that all light was blocked out. The treatment groups remained either in the dark or the light until the end of the normal photoperiod at 19:00 at which point the dishes in the dark were returned to the irradiation chamber.

At this time, half the embryos were removed for DNA analysis. After removing the water from a dish, the embryos were transferred into 1.5 mL Eppendorf microfuge tubes using a rubber spatula. Any remaining water was removed with a Pasteur pipette. The samples were quick frozen in liquid nitrogen and stored at -70ºC until DNA extraction was performed. For the remaining days of the study periods, the embryos were kept in the irradiation chamber under the 14L:10D photoperiod until all the embryos had hatched. After hatching, the larvae were categorized as described above.

Table I: PAR and UVR schedule for each of the treatment groups during the pre-illuminated photorepair experiments. The embryos were incubated on a 14L:10D photoperiod. From 19:00 to 05:00 of the next day, the embryos were incubated in the water baths in darkness.

Treatment group	Day 1 Fert. to 19:00	Day 2 05:00 - 19:00	Day 3			Day 4 to hatching 05:00 – 19:00
			05:00-09:00	09:00-13:00	13:00-19:00	
LC *(light control)*	PAR UV-A	PAR UV-A	PAR UV-A	PAR UV-A	PAR UV-A	PAR UV-A
LE *(light experimental)*	PAR UV-A	PAR UV-A	PAR UV-A	PAR UV-A +UV-B	PAR UV-A	PAR UV-A
DC *(dark control)*	PAR UV-A	PAR UV-A	PAR UV-A	PAR UV-A	Dark	PAR UV-A
DE *(dark experimental)*	PAR UV-A	PAR UV-A	PAR UV-A	PAR UV-A +UV-B	Dark	PAR UV-A

Non-illuminated trials

These experiments proceeded in the same fashion as the illuminated experiments however PAR and UV-A were removed at approximately 24 hours post-fertilization. The treatment of the embryos in the different groups is summarized in Table II. The embryos remained in darkness until 09:00 when irradiation with only UV-B began. After the four-hour irradiation period, the light groups received phototherapy (PAR and UV-A) until 19:00, the normal end of the photoperiod and the dark groups were placed into the dark box until 19:00 when they were returned to the irradiation chamber.

Performed in the same way as the illuminated experiments, half the embryos were removed and quick frozen for further DNA analysis.

Data Analysis

For each dish, fertilized egg number was determined by summing the number of all hatchlings and the number of dead eggs in days 2, 3 and 4. The fertilization rate for each dish and each female fish was determined by dividing the fertilized eggs by the sum of the fertilized eggs and infertile eggs. The fraction of anatomically normal larvae was determined as a percentage of the number of viable eggs on day 3 (dead eggs from days 2 and 3 subtracted from fertilized eggs). These data were arcsine square root transformed before analysis using SPSS software. The transformed data was subjected to two-way full factorial analysis of variance (ANOVA) with Type III sum of squares. The dependent variable was the transformed percent normal larvae, treatment was set as the fixed factor and the random factor was female fish. A Satterthwaite approximation was employed when calculating degrees of freedom due to the unbalanced number of dishes per female fish. Tukey's Honestly Significantly Difference (HSD) multiple comparison post-hoc test was applied

Table II: PAR and UVR schedule for each of the treatment groups during the photorepair experiments without pre-illumination. The embryos were incubated on a 14L:10D photoperiod. From 19:00 to 05:00 of the next day, the embryos were incubated in the water baths in darkness.

Treatment group	Day 1 Fert. to 19:00	Day 2		Day 3			Day 4 to hatching 05:00 – 19:00
		05:00-12:00	12:00-19:00	05:00-09:00	09:00-13:00	13:00-19:00	
LC *(light control)*	PAR UV-A	PAR UV-A	Dark	Dark	Dark	PAR UV-A	PAR UV-A
LE *(light experimental)*	PAR UV-A	PAR UV-A	Dark	Dark	UV-B	PAR UV-A	PAR UV-A
DC *(dark control)*	PAR UV-A	PAR UV-A	Dark	Dark	Dark	Dark	PAR UV-A
DE *(dark experimental)*	PAR UV-A	PAR UV-A	Dark	Dark	UV-B	Dark	PAR UV-A

when the interaction term between fish and treatment was not significant. M. D. Wiegand established the initial method for the analysis of survival data.

DNA Damage Analysis

The basis of the DNA damage analysis was the endonuclease sensitive site (ESS) assay. The assay uses endonuclease V, a base excision enzyme from the T4 bacteriophage, to determine the frequency of CPDs in a DNA sample. T4 endonuclease V produces a single-stranded nick in the DNA strand through a two-step reaction involving the cleavage of the N-glycosidic bond at the apyrimidinic site and the cleavage of the phosphodiester bond by β-elimination (Fuxreiter *et al.* 1999). The T4 endonuclease V finds the damaged site by processively scanning the DNA molecules, which is similar to the mechanism used by the restriction endonuclease EcoRI and *Escherichia coli lac* repressor protein (Gruskin and Lloyd 1986).

Because the nick produced is single-stranded, denaturing conditions are required to separate the strands of DNA. Formaldehyde, formamide, sodium hydroxide or urea can be used to denature the DNA and avoid renaturation (Drouin *et al.* 1996). By maintaining denaturing conditions before and during electrophoresis, the migration of single-stranded fragments can be measured. Incubation of DNA samples containing CPDs with T4 endonuclease V will show the increased migration of shorter molecular weight fragments. The shorter fragments are a result of increased fragmentation due to an increased frequency of CPDs.

Calf thymus DNA trials

Before initiating digestion of goldfish samples, trials with calf thymus DNA were conducted to ensure the ESS assay was a reasonable and functional method of detecting CPDs. The protocol used was adapted from Drouin (1997). A 200 μg/mL calf thymus

DNA (Sigma) solution was prepared by dissolving the DNA in irradiation buffer (50 mM Tris-HCl pH 7.6, 1 mM EDTA, 50 mM NaCl, 1 mM β-mercaptoethanol) that was later used for digestion. A 1.75 mL fraction of the 200 μg/mL DNA solution was diluted to 5 mL. The diluted DNA sample (70 μg/mL) was irradiated to a dose of 1033.8 J/m^2 UVC from two germicidal bulbs.

After irradiation, samples from the irradiated and non-irradiated DNA were digested with two different amounts of T4 endonuclease V (Interscience, Inc.). Details of the digestion protocol and ESS assay can be found in Table III. The DNA was digested with endonuclease for one hour at 37ºC. After digestion, the DNA was precipitated by adding sodium acetate and 95% ethanol and incubating at –70ºC for 60 minutes. The DNA was sedimented, air dried and resuspended in ddH_20. The specific protocol for DNA precipitation and preparation for alkaline electrophoresis is detailed in Appendix B. To denature the DNA, an aliquot of the DNA was incubated for 20 minutes at room temperature with the denaturing loading buffer and denaturing solution (100 mM NaOH; 4 mM EDTA). The denatured DNA was electrophoresed (Wide Mini Sub® Cell GT, Power Pac 300; Bio-Rad) for 12 hours at 0.4 V/cm at 4ºC in a 1% alkaline agarose gel (Certified™ Molecular Biology Agarose, Bio-Rad). After electrophoresis, the gel was first neutralized in a Tris-buffered solution (0.1 M Tris, pH 7.5-8.0) for 20–30 minutes and stained in ethidium bromide (0.5 μg/mL) for 20–30 minutes. Photographing the gel on Gel Doc 2000 (Bio-Rad) under UV illumination allowed analysis the distribution of fluorescence by Quantity One software (Bio-Rad). Data was exported to Excel (Microsoft Office) for further analysis.

Table III: Digestion protocol for calf thymus DNA divided into four groups to determine if T4 endonuclease was functional. Irradiated DNA (70μg/mL) was irradiated using one germidical lamp to a dose of 1033 J/m2. Two different amounts of enzyme were used to determine the most effective concentration of endonuclease. Samples were digested for 1 hour at 37°C.

	DNA	Enzyme
No UV; no T4 endonuclease	50 μL 200 μg/mL non-irradiated DNA	0 units
No UV + T4 endonuclease	50 μL 200 μg/mL non-irradiated DNA	4 units
		8 units
UV; no T4 endonuclease	143 μL 70 μg/mL irradiated DNA	0 units
UV + T4 endonuclease	143 μL 70 μg/mL irradiated DNA	4 units
		8 units

Genomic goldfish DNA trials

Phenol-chloroform extractions (Maniatis *et al.* 1982) were performed to extract DNA from the experimental groups that received no PAR and UVA prior to irradiation. Details of the extraction can be found in Appendix C. A urea homogenizing buffer was adapted from Ahmed and Setlow (1993) who discovered that this buffer provided consistent extraction of high molecular weight DNA. After extraction, the amount of DNA recovered in each extraction was quantified. Using known quantities (0.5, 1.0, 2.0 and 3.0 µg) of calf thymus DNA as standards, the relative quantity of DNA from the extractions was be determined. Calf thymus standards and goldfish extractions were digested with *Eco*RI (Roche Applied Science) for one hour in order to fragment the DNA. RNA contamination was removed by RNase (Roche Applied Science) that was also added during the one hour incubation. The fragmented genomic DNA would migrate into the agarose gel further during electrophoresis. Standards, DNA molecular weight marker X (0.07-12.2 kbp; Roche Applied Science), and extracts were electrophoresed on a 1% agarose gel for 90 minutes at 2.4 V/cm after which the gel was stained for 20 minutes with ethidium bromide (0.5 µg/mL). Using Quantity One software (Bio-Rad), the intensity of the lanes was compared. The average fluorescence intensity for the standards was determined and used to prepare a standard curve to extrapolate the amount of DNA extracted from the goldfish embryos. Using the phenol-chloroform method of extraction, it was possible to isolate 24.1 ± 2.2 µg DNA from the embryos.

When the amount of DNA extracted from each sample was determined, the samples were precipitated with 3M sodium acetate and 95% ethanol kept at -70°C. After incubation at –70°C for one hour, the precipitated DNA was spun down and resuspended

in digestion buffer (50 mM Tris-HCl pH 7.6, 1 mM EDTA, 50 mM NaCl, 1 mM β-mercaptoethanol) for digestion by T4 endonuclease V (Drouin 1997). Ten micrograms of goldfish DNA was digested with six units of T4 endonuclease V for 2 hours at 37°C. Exact protocols for the digestion can be found in Appendix D. The neutralized and stained gels were photographed and scanned as in the calf thymus trials. The data from the distribution of fluorescence was exported to Excel for further analysis.

Data Analysis

When analyzing the scanned photograph of the gel taken on the Gel Doc 2000 camera, the total number of pixels or the integrated area under the curve for a graph of the fluorescence intensity against relative migration distance corresponds to the total amount of DNA loaded into the sample well. The median migration distance, or the midpoint of the DNA mass, was converted into median molecular length (L_{med}) using the standard curve from the DNA standard ladder used on the gel. The median molecular length was then converted to average molecular length (L_n) using this formula (Sutherland and Shih 1983):

$$L_n = 0.6 \times L_{med}$$

The number of ESS per base, which corresponds to the number of CPDs per base, was calculated using

$$\frac{ESS}{base} = \frac{1}{L_{n(+UV)}} - \frac{1}{L_{n(-UV)}}$$

Where $L_{n(+UV)}$ is the average molecular length of sample irradiated with UV-B and $L_{n(-UV)}$ is the average molecular length of sample not exposed to UV-B (Sutherland and Shih 1983). The conversion of the data is adapted from the analysis by Sutherland and Shih (1983). Since the endonuclease specifically binds to CPDs, the number of CPDs is equal to the number of breaks (Sutherland and Shih 1983).

RESULTS

Embryo survival data

The average fertilization rate was 96.1 ± 0.5%. The two way, full factorial ANOVA for the arcsine square root transformed percent anatomically normal larvae from the illuminated trials computed *p*-values were 0.692 and 0.256 for the effect of treatment and effect of female donor fish, respectively. Therefore, no significant difference exists between the groups at the 5% level of significance. The transformed percent anatomically normal larvae data, referred to as survival data, are presented in Figure 2. The average percentage of anatomically normal larvae was 73 ± 3%.

In contrast, in the non-illuminated trials, the dark experimental group experienced a drastic decrease in survival, approximately 42%, compared to the other experimental groups (Figure 2). A two-way ANOVA testing at $p<0.05$ indicated a difference in survival between treatments. Any fish effect (interaction variable), which refers to variation based on female donor fish, had no significant effect on survival. A Tukey's HSD test confirmed that the dark experimental group is significantly different than the other groups (Table IV).

Between the illuminated and non-illuminated trials, the survival of the control groups differs by approximately 22%. The decrease in survival in the non-illuminated trials might be attributed to removal of visible and UV-A radiation possibly impairing development. The non-illuminated experiments were performed with the last eggs spawned in the summer therefore the quality of the eggs may have declined due to the late spawning. Goldfish usually spawn in nature during the spring (Wiegand, personal communication). It would be of interest to observe whether the specific types of abnormalities had changed in frequency from the beginning of the summer.

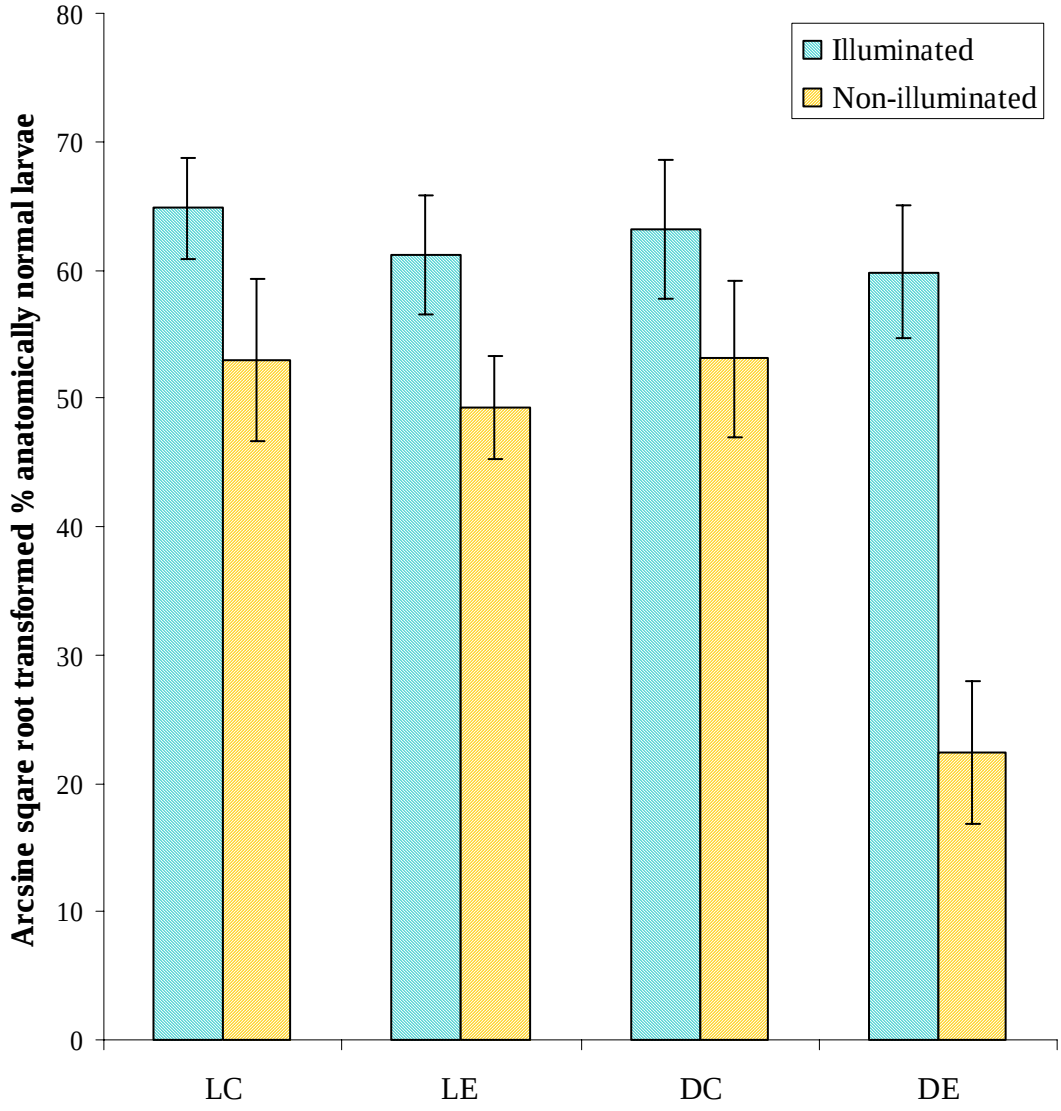

Figure 2: The effectiveness of treatment in illuminated and non-illuminated photorepair experiments on the arcsine square root transformed percentage of anatomically normal larvae (± standard error). Abbreviations represent the four treatment groups: LC = light control, LE = light experimental, DC = dark control, DE = dark experimental. No significant difference ($p<0.05$) exists between the groups in the illuminated trials, whereas the survival of the DE group significantly decreased in the non-illuminated trials.

Table IV: Results of Tukey's HSD test showing pairwise comparisons of goldfish embryo survival between treatment groups in non-illuminated photorepair experiments.

Treatment pairwise comparisons	*p*-value
LC and LE	0.956
LC and DC	1.000
LC and **DE***	**0.001**
LE and DC	0.952
LE and **DE***	**0.005**
DC and **DE***	**0.001**

* Mean difference is significant at 5% level

Calf thymus ESS assay

The densitometric scan of the distribution of the intensity of fluorescence is shown in Figure 3. Integration of fluorescence intensity was used to determine the migration distance for the DNA sample. The sample that migrated furthest was the sample that was irradiated and treated with T4 endonuclease V. The other samples either received no UVR treatment and/or were not digested with T4 endonuclease V. Even by visual assessment of the shape of the curves, the migration pattern for the samples is different.

Specifically, increased migration distance indicates a decrease in molecular weight. In these experiments, cleavage at CPDs by T4 endonuclease V caused a decrease in the length of the DNA fragments. The analysis of this trial could not proceed past determining the median migration distance of the DNA sample because the DNA ladder had diffused and become faint when the gel was visualized by UV light.

Goldfish ESS assay

Prior to digesting the extracted goldfish DNA, the samples were quantified using calf thymus standards. A densitometric scan of the fluorescence intensity was analyzed by averaging the fluorescence intensity of the calf thymus DNA standards to construct a standard curve. The approximate concentration of the goldfish samples was obtained by extrapolating from the standard curve using the average fluorescence intensity. Instead of using averages to determine quantity, the area under the curve should have been integrated; however, at the time of quantification, a method of integration had not yet been considered. The method of quantification that was used was probably not sufficiently accurate and might have resulted in inconsistent amounts of sample loaded in the ESS assay. Only extracted DNA from non-illuminated trials were used for the ESS assay.

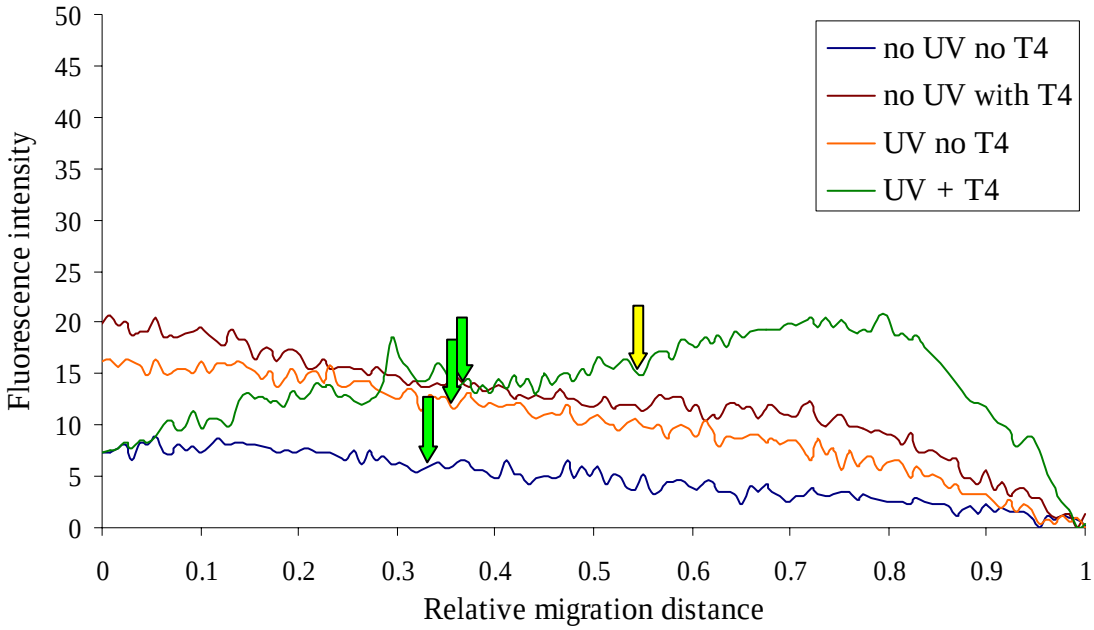

Figure 3: Profile of fluorescence intensity distribution over the migration distance of calf thymus DNA. Green arrows represent median migration distance traveled by the DNA samples of the treatment groups: no UV, no T4 endonuclease V; no UV, plus T4 endonuclease V; UV, no T4 endonuclease V. The yellow arrow signifies the treatment groups that was irradiated with UVR and digested with T4 endonuclease V.

Similar to the calf thymus experiments, the stained agarose gel was scanned to obtain the distribution of fluorescence intensity over relative migration distance of the sample (Figure 4). Exporting the fluorescence data into Excel allowed integration of the area under the curve through counting the squares of a fine grid underneath the curve. As the squares were counted, the cumulative area was tabulated. The total number of squares is equivalent to the integrated area, or the total DNA loaded into the well. The median point of the DNA sample, equal to the median migration distance, was determined by dividing the total by 2. The median migration could then be converted into average molecular length and this was used to calculate frequency of ESS per base, as specified earlier.

Five agarose gels were analyzed in this manner despite six agarose gels being electrophoresed. One gel was discarded from analysis because only one band was detectable when visualized under UV light. In order to analyze samples of similar DNA concentration, samples whose bands were too faint or too intense also were eliminated from analysis to ensure consistent concentration for comparison. A randomized block model was used to attempt statistical determination of significance for the effect of treatment on the average molecular length of the DNA fragments. For analysis, the values of average molecular length were blocked by fish and gel. The data from the gels was not combined due to sufficiently disparate gel conditions. By using this design, data from fish 230 and 231 were discarded due to insufficient sample size. Using the randomized block model, an ANOVA testing at the 5% level of significance reveals a significant difference in the effect of treatment. Significant difference in the DE treatment group is revealed by Tukey's HSD multiple comparisons post-hoc test. Data from each fish is summarized in Table V.

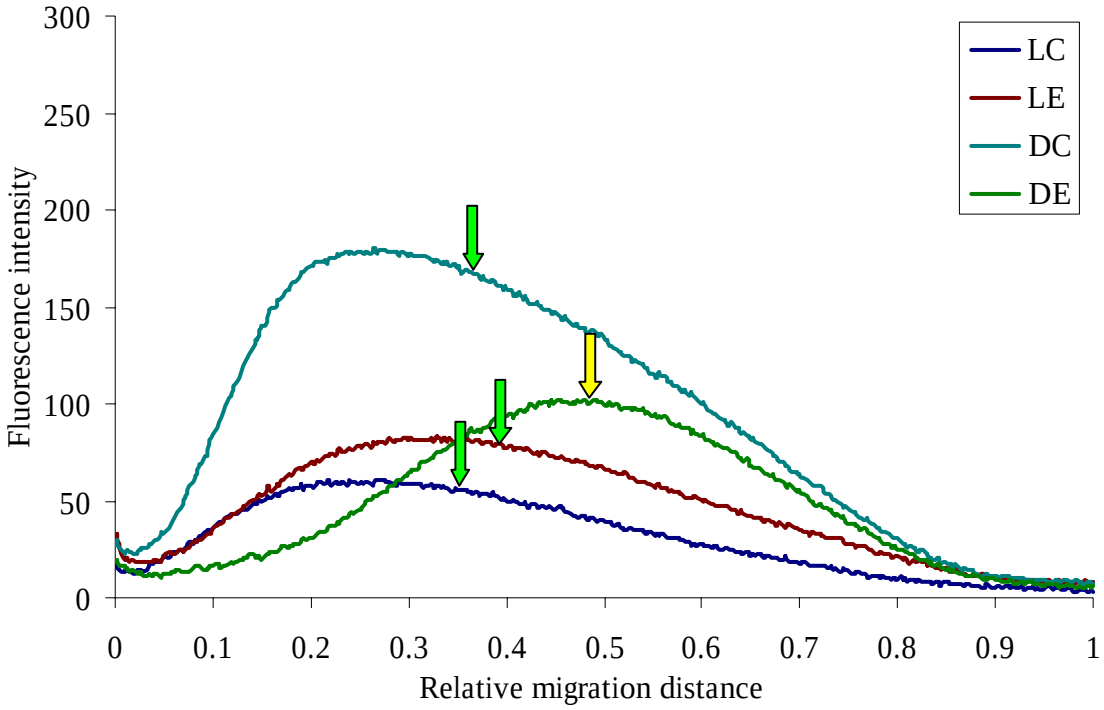

Figure 4: Densitometric scan of the distribution of fluorescence in relationship to migration distance for goldfish gel 3. Green arrows represent median migration distance for the light control, light experimental and dark control treatment groups. The yellow arrow indicates the median migration distance of the dark experimental treatment groups.

Table V: Randomized block model ANOVA and Tukey's HSD multiple comparison tests results for goldfish endonuclease sensitive site (ESS) assay. Data were blocked by gel and fish, and samples with too little or too much fluorescence intensity were eliminated. Fish were separated based on assigned numbers.

Fish	Source of variation	*p*-value	Pairwise comparison	*p*-value
226	Treatment*	**0.024**	LC and LE	1.00
	Gel	0.328	LC and DC	0.996
			LC and **DE***	**0.029**
			LE and DC	0.991
			LE and **DE***	**0.027**
			DC and **DE***	**0.034**
227	Treatment	0.072	LC and LE	0.596
	Gel	0.305	LC and DC	0.928
			LC and DE	0.186
			LE and DC	0.864
			LE and **DE****	**0.061**
			DC and **DE****	**0.097**
228	Treatment*	**0.005**	N/A***	N/A
	Gel*	**0.014**		

*Significant at 5% level.
**Marginally significant at 10% level.
*** Post-hoc test not performed due to insufficient sample size

Figure 5 shows the average molecular length (± standard error) according to treatment group for each gel. Any column without error bars is a case where only one sample was suitable for analysis. On any gel, some lanes with samples did not have sufficient DNA to produce a signal detectable by the camera. Therefore, at times only one sample from a treatment group was detectable. The dark experimental groups in gels 2, 3 and 4 exhibit a decrease in the average molecular length of the DNA fragments and the remaining three groups have similar fragment lengths. The values from gel 1 and 5 indicate no particular pattern in the length of DNA fragments. In these cases, the non-specific breakage of the genomic DNA strands caused by shearing during extraction or quantification would cause haphazard patterns in fragment length.

The average molecular length data is more meaningful when combined with the examination the frequency of ESS per base. Figure 6 shows the effect of phototherapy or dark treatment on the calculated frequency of ESS/base, which is equivalent to the number of CPDs present per base of DNA. Negative values in gels 1 and 5 suggest that more damage due to dimers persisted in non-irradiated samples than irradiated samples. Since CPDs are induced by UVR, it is unlikely that the control groups would contain any CPDs; therefore, the apparent frequency of ESS/base and average molecular length is attributed to mechanical shearing and degradation of the genomic DNA during extraction. In gel 2, 3 and 4, the frequency of ESS in the samples exposed to phototherapy approximately 90%, 68% and 63%, respectively, lower than in the samples that were placed immediately into darkness. The repair processes present in the organisms were able to remove at least two thirds of the damage over a 6-hour period.

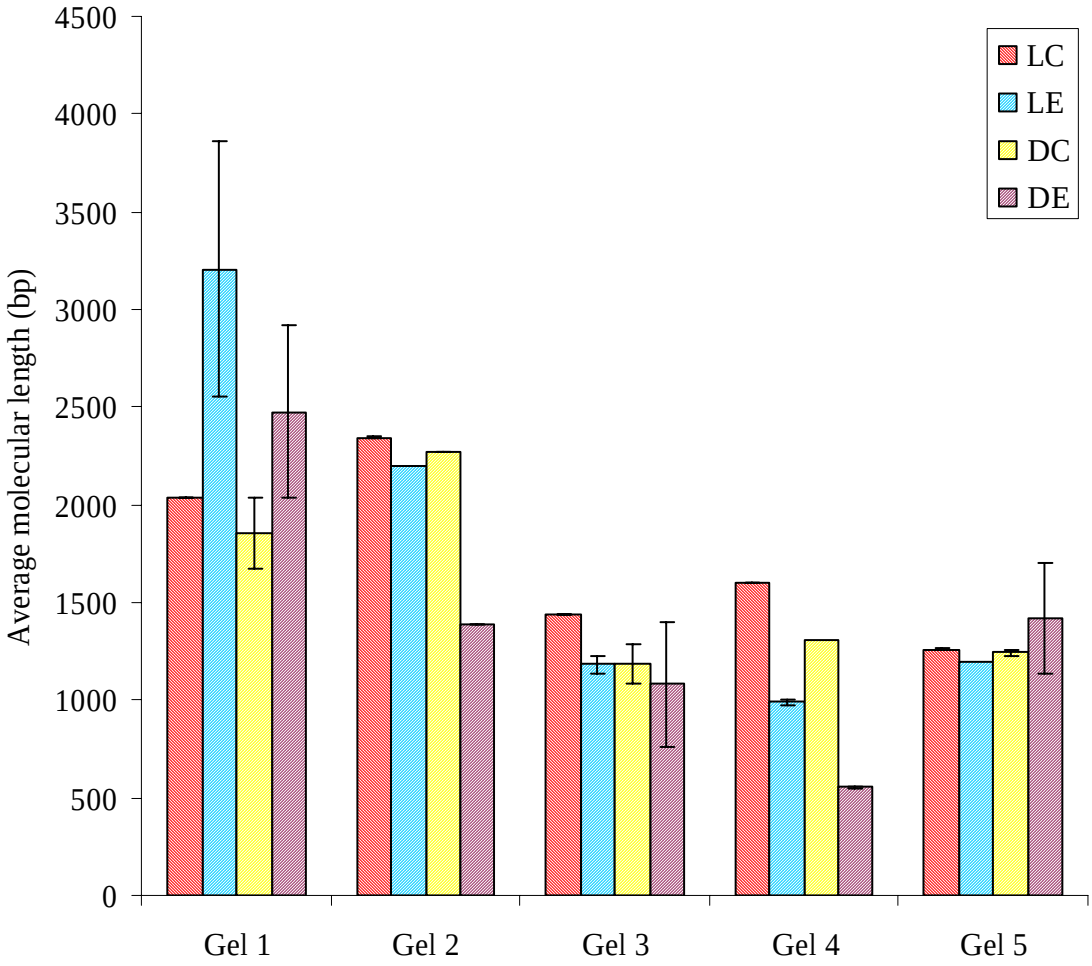

Figure 5: Average molecular length of goldfish DNA samples digested with T4 endonuclease V and electrophoresed under alkaline conditions. Errors bars, when present, are ± standard error. The results are grouped by gel number since the individual gel conditions were too different for comparisons between gels to be valid.

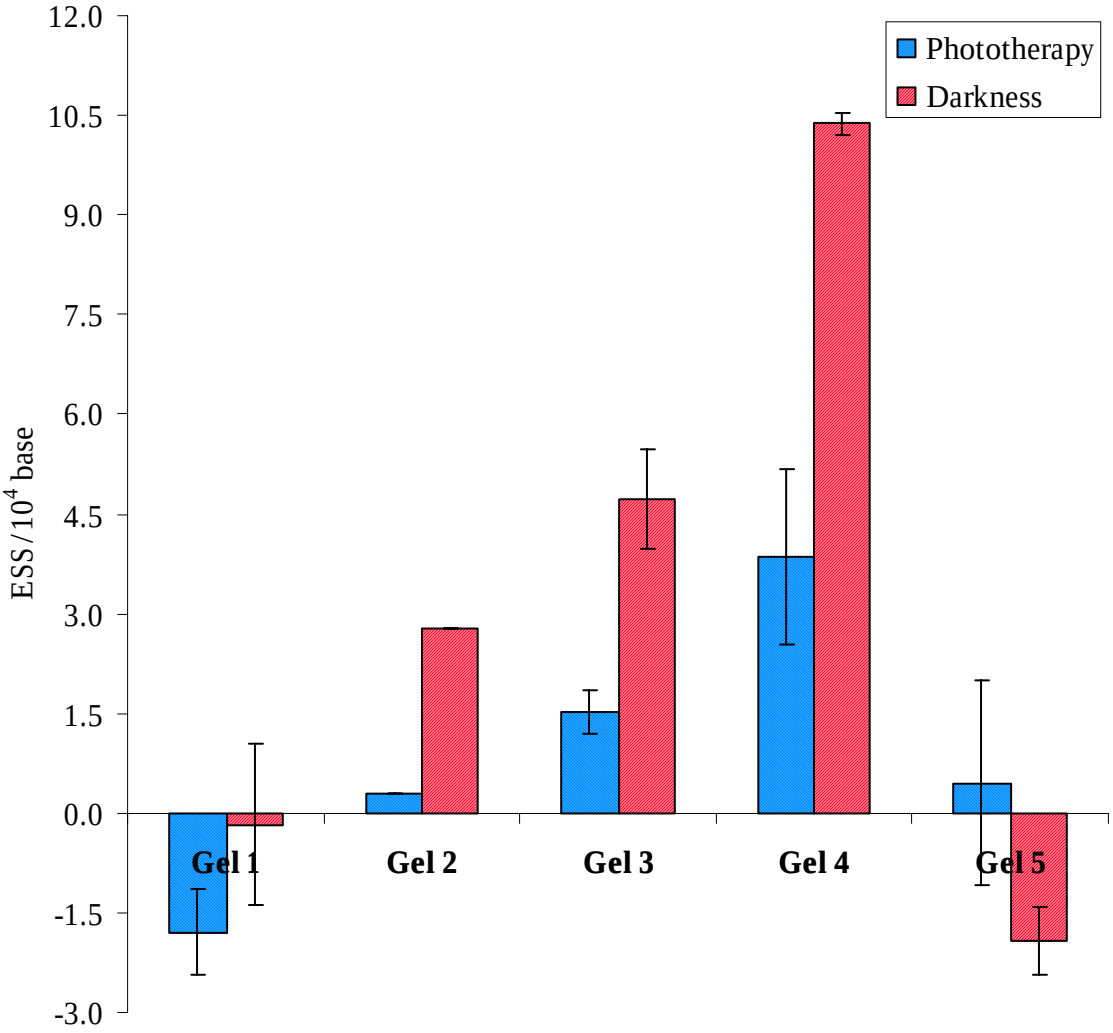

Figure 6: The frequency of endonuclease sensitive sites (ESS) per base in goldfish DNA samples, grouped by gel number, that have been digested by T4 endonuclease V. The frequency of ESS is directly proportional to the amount of UV-induced dimers. Errors bars represent ± standard error.

DISCUSSION

Presence of light enables goldfish embryos to withstand the damaging effects of UV exposure. In natural lighting regimes, where PAR and UV-A are present, survival is not significantly changed upon UV-B irradiation. However, the removal of PAR and UV-A prior to and during UV-B exposure significantly reduces survival. The reduced percent survival in the irradiated groups without phototherapy accompanies a higher frequency of CPDs; therefore, dimers must play a major role in the killing of cells. Since CPDs are specifically repaired by photolyase, photoreactivation is the dominant mechanism of repair, surpassing dark repair, which alone did not affect the survival of the embryos. The frequency of CPDs present in the DNA is the net result of both the damaging and repair processes. Concurrent and preceding light reversed enough damage during irradiation so that sublethal frequencies of CPDs were not detectable.

Thuen (2002) suggested that critical processes for DNA protection and repair begin after the second day of development. Latent development of such processes would explain the susceptibility of the embryos to UV-induced damage on day 2. In the light of the reported experiments, it is suggested that the processes that develop during day 2 are light dependent since the sensitivity to UVR was carried over to the third day of development when light was removed at 24 hours post-fertilization. Day 3 had been established as a time when the embryos were resistant to UV damage (Thuen 2002); however, removal of visible light and UV-A induced vulnerability to UV-B on day 3. The developmental stage dependence of UVR sensitivity in the embryos supports the “one bad day” hypothesis that states even brief exposure to UVR during a critical stage of development will cause significant morbidity and mortality (Vincent and Neale 2000).

It has been shown that the response to UVR in embryos is not only dependent on the dose and flux of radiation, but also dependent on the developmental stage of the embryos at the time of irradiation (Dethlefsen *et al.* 2001). In the goldfish embryos, the damaging effects were most severe when PAR and UV-A were removed 24 hours post-fertilization. At this point in development, the optic vesicles, optic cup and lens are developing (Kajishima 1960). Irradiation with UV-B commenced at 48 hours post-fertilization, a time when melanophores and pigmentation in the eyes begin to appear (Kajishima 1960). UV-B exposure impairs important functions active during embryo development, such as gene expression.

However, UVR exposure does not only interfere with gene expression. Studies on zebrafish (*Brachydanio rerio*) embryos (Strähle and Jesuthasen 1993) indicate that UV irradiation affects other processes vital to embryo development. During the process of epiboly, the blastoderm spreads over the yolk mass, seemingly moved by the yolk syncytial layer (YSL), a multi-nuclear cytoplasmic layer between the yolk and blastoderm. The YSL epibolizes faster than and independent of the blastoderm (Strähle and Jesuthasen 1993). UVR interferes with epiboly when embryos are irradiated either during meroblastic cleavage of the zygote or during epiboly stages. Irradiation destroys the microtubule arrays that form in the cortical layer of the yolk cytoplasm responsible for YSL movement, thus reducing the velocity of epiboly (Strähle and Jesuthasen 1993). Because epiboly plays an integral role during the period of axis specification, these early stages of development are UV sensitive in zebrafish embryos (Strähle and Jesuthasen 1993). Interference with microtubules might account for goldfish embryo sensitivity in the first 12 hours post-fertilization; however, by 24 hours post-fertilization the embryos has developed into a more advanced organism

(Kajishima 1960) which begs the question if the mechanism of sensitivity changes based on developmental stage.

Studies in the pattern of photolyase expression in *Drosophila* (Todo *et al.* 1994) and medaka (Uchida *et al.* 1997) have revealed that the photorepair enzymes, CPD photolyase in *Drosophila* and (6-4) photolyase in medaka, are maternal effect genes. In *Drosophila*, photolyase is stored in the eggs and ovaries. In insects, the evolution of photolyase as a maternal gene was propagated due to the necessity of quick and efficient DNA repair in early egg stages as a defence against solar UVR (Todo *et al.* 1994). It is possible in goldfish that the lag period in UVR resistance exists in day 2 due to the dilution of maternal photolyase. On day 1, the embryos contain and rely on maternal photolyase for repair, but as cell division occurs, the maternal photolyase dilutes and it is not until day 3 that the embryos begin producing their own photolyase. Further studies on the expression of the photolyase gene and the activity of the protein in the ovaries of the female donor fish and the embryos during all stages of development are required to determine the mechanism of vulnerability.

Rapid removal of CPDs in DNA results from the enhanced stability of photoreactivation by CPD photolyase, as opposed to (6-4) photolyase (Uchida *et al.* 1997). In larval northern anchovy, CPD repair dominates since the photolyase gene is constitutively expressed, even in darkness. The repair is efficient enough that no CPD accumulation occurred during the course of the four-day experiment (Vetter *et al.* 1999). In 30 minutes of incubation in fluorescent light, Funayama *et al.* (1994) found that 85% of CPDs were removed from the tail fin cells of medaka. The degree of dark repair was determined by measuring the frequency of the dimers before and after 6 hours of dark

incubation. Dark repair repaired 40% of the CPDs and 80% of the (6-4)PPs (Funayama *et al.* 1994). Twenty minutes of phototherapy treatment was sufficient to repair 70% of the CPDs in RBCF-1 cells, while fewer than 20% of CPDs were removed in RBCF-1 cells incubated in the dark for the same length of time (Yasuhira *et al.* 1991).

The amount of dark repair in goldfish embryos is unknown and future work should include determining the degree of dark repair. Dark repair can be measured by removing embryos at the beginning and the end of the phototherapy or dark treatment period and used as correction factor for groups receiving phototherapy. Generally, NER removes (6-4)PPs faster than CPDs (Koehler *et al.* 1996); however, to establish this trend in goldfish, different techniques in damage detection could be adopted. The ESS assay sufficiently established relative photorepair ability in goldfish embryos despite any dilution effects due to rapidly increasing cell number and cell loss due to apoptosis. However, non-specific breakage in the high molecular weight genomic DNA falsely increased the values for dimer frequency, reducing the sensitivity of the detection technique. Alternatively, Vetter *et al.* (1999) has developed a highly sensitive technique using antibodies raised against CPDs to measure sublethal damage in small samples.

The amount and dosage of photorepair necessary for recovery of survival remains to be determined; however, in the future, more sensitive techniques than the ESS assay should be employed. Time becomes an important factor in repair when considering that the nucleosome structure in genomic DNA exerts site-specific constraints on repair. Despite the limited accessibility of the DNA, the dynamic nature of nucleosomes *in vivo* allows repair to take place over time as the damage eventually becomes more accessible (Schieferstein and Thoma 1998). The DNA strand must also be flexible enough to support

the bound photolyase enzyme and the repair reaction (Thoma 1999). Therefore, accounting for the length of time needed to remove the majority of CPDs would provide insight into the minimum requirements for survival of embryos.

CONCLUSIONS

1. Exposing goldfish embryos to UV-B at 48 hours post-fertilization when light has been removed at 24 hours post-fertilization induces vulnerability at a time embryos are normally resistant to the damaging effects of UVR.

2. Persistence of cyclobutane pyrimidine dimers correlates to decreased survival in embryos, indicating that CPDs are a major factor in cell killing.

3. Goldfish embryos are capable of photorepair of CPDs.

REFERENCES CITED

Ahmed, F. E. and R. B. Setlow. 1993. Ultraviolet radiation-induced DNA damage and its photorepair in the skin of the platyfish *Xiphophorus*. Cancer Research 53: 2249-2255.

Applegate, L. A. and R. D. Ley. 1988. Ultraviolet radiation-induced lethality and repair of pyrimidine dimers in fish embryos. Mutation Research 198: 85-92.

Aubert, C., Vos, M. H., Mathis, P., Eker, A. P. M., and K. Brettel. 2000. Intraprotein radical transfer during photoactivation of DNA photolyase. Nature 405: 586-590.

Carell, T., Burgdorf, L. T., Kundu, L. M., and M. Cichon. 2001. The mechanism of action of DNA photolyases. Current Opinion in Chemical Biology 5: 491-498.

Dethlefsen, V., von Westernhagen, H., Tug, H., Hansen, P. D., and H. Dizer. 2001. Influence of solar ultraviolet-B on pelagic fish embryos: osmolality, mortality and viable hatch. Helgoland Marine Research 55: 45-55.

Drouin, R. 1997. Optimal conditions for digesting genomic DNA with T4 endonuclease V. Epicenter Forum. V 4 @ www.epicenter.com/fv-lev.asp.

Drouin, R., Gao, S., and G. P. Holmquist. 1996. Agarose gel electrophoresis for DNA damage analysis. *In* Technologies for detection of DNA damage and mutations. *Edited by* G. P. Pfeifer. Plenum Press, New York, pp. 37-43.

Fox, M. E., Feldman, B. J., and G. Chu. 1994. A novel role for DNA photolyase: Binding to DNA damaged by drugs is associated with enhanced cytotoxicity in *Saccharomyces cerevisiae*. Molecular and Cellular Biology 14: 8071-8077.

Funayama, T., Mitani, H., Ishigaki, Y., Matsunaga, T., Nikaido, O., and A. Shima. 1994. Photorepair and excision repair removal of UV-induced pryimidine dimers and (6-4) photoproducts in the tail fin of the Medaka, *Oryzia latipes*. Journal of Radiation Research 35: 139-146.

Fuxreiter, M., Warshel, A., and R. Osman. 1999. Role of active site residues in the glycosylase step of T4 endonuclease V. Computer simulation studies on ionization states. Biochemistry 38: 9577-9589.

Gruskin, E. A. and R. S. Lloyd. 1986. The DNA scanning mechanism of T4 endonuclease V. Effect of NaCl concentration on processive nicking activity. Journal of Biological Chemistry 261: 9607-9613.

Husain, I., Sancar, G. B., Holbrook, S. R., and A. Sancar. 1987. Mechanism of damage recognition by *Escherichia coli* DNA photolyase. Journal of Biological Chemistry 262: 13188-13197.

Jang, Y. K., Wang, L., and G. B. Sancar. 1999. RPH1 and GIS1 are damage-responsive repressors of PHR1. Molecular and Cellular Biology. 19: 7630-7638.

Kajishima, T. 1960. The normal development stages of the goldfish *Carassius auratus*. Japanese Journal of Ichthyology. 8: 20-28.

Koehler, D. R.., Courcelle, J., and P. C. Hanawalt. 1996. Kinetics of pyrimidine(6-4) pyrimidone photoproduct repair in *Escherchia coli*. Journal of Bacteriology. 178: 1347-1350.

Komori, H., Masui, R., Kuramitsu, S., Yokoyama, S., Shibata, T., Inoue, Y., and K. Miki. 2001. Crystal structure of thermostable DNA photolyase: pyrimidine-dimer recognition mechanism. Proceedings of the National Academy of Science USA 98(24): 13560-13565.

Komura, J.-I., Mitani, H., Nemoto, N., Ishikawa, T., and A. Shima. 1991. Preferential excision repair and non-preferential photoreactivation of pyrimidine dimers in the c-*ras* sequence of cultured goldfish cells. Mutation Research, DNA Repair 254: 191-198.

Maniatis, T., Fritsch, E. F., and J. Sambrook. 1982. Molecular Cloning: A Laboratory Manual. Cold Spring Harbor Laboratory, USA, pp. 545.

Medvedev, D., and A. A. Stuchebrukhov. 2001. DNA repair mechanism by photolyase electron transfer path from the photolyase catalytic cofactor FADH- to DNA thymine dimer. Journal of Theoretical Biology 210: 237-248.

Mitani, H., and A. Shima. 1995. Induction of cyclobutane pyrimidine dimer photolyase in cultured fish cells by fluorescent light and oxygen stress. Photochemistry and Photobiology 61: 373-377.

Mitani, H., Uchida, N., and A. Shima. 1996. Induction of cyclobutane pyrimidine dimer photolyase in cultured fish cells by UVA and blue light. Photochemistry and Photobiology. 64: 943-948.

Mitchell, D. L., and R. S. Nairn. 1989. The biology of the (6-4)photoproduct. Photochemistry and Photobiology 49: 805-819.

Nishigaki, R., Mitani, H., and A. Shima. 1998. Evasion of UVC-induced apoptosis by photorepair of cyclobutane pyrimidine dimers. Experimental Cell Biology 244: 43-53.

Ozer, Z., Reardon, J. T., Hsu, D. S., Malhotra, K., and A. Sancar. 1995. The other function of DNA photolyase: simulation of excision repair of chemical damage to DNA. Biochemistry. 34: 15886-15889.

Roy, S. 2000. Strategies for the minimisation of UV-induced damage. *In* The effects of UV radiation in the marine environment. *Edited by* S. de Mora, S. Demers and M. Vernet. Cambridge University Press, London, pp. 177-205.

Schieferstein, U. and F. Thoma. 1998. Site-specific repair of cyclobutane pyrimidine dimers in a positioned nucleosome by photolyase and T4 endonuclease V *in vitro*. The EMBO Journal. 17: 306-316.

Sebastian, J. and G. B. Sancar. 1991. A damage-responsive DNA binding protein regulates transcription of the yeast DNA repair gene PHR1. Proceedings of the National Academy of Science USA 88: 11251-11255.

Setlow, R. B. 2002. Shedding light on proteins, nucleic acids, cells, humans and fish. Mutation Research. 511: 1-14.

Shima, A. and R. B. Setlow. 1984. Survival and pyrimidine dimers in cultured fish cells exposed to concurrent sun lamp ultraviolet and photoreactivating radiations. Photochemistry and Photobiology 39: 49-56.

Steeger, H.-U., Freitac, J. F., Wiemer, M., and R. J Paul. 2001. Effects of UV-B radiation on embryonic, larval and juvenile stages of North Sea plaice (*Pleuronectes platessa*) under simulated ozone-hole conditions. Helgoland Marine Research 55: 56-66.

Strähle, U. and S. Jesuthasen. 1993. Ultraviolet irradiation impairs epiboly in zebrafish embryos: evidence for a microtubule-dependent mechanism of epiboly. Development 119: 909-919.

Sutherland, B. M. and A. G. Shih. 1983. Quantitation of pyrimidine dimer contents of nonradioactive deoxyribonucleic acid by electrophoresis in alkaline agarose gels. Biochemistry 22: 745-749.

Sweet, D. H., Jang, Y. K., and G. B. Sancar. 1997. Role of UME6 in transcriptional regulation of a DNA repair gene in *Saccharomyces cerevisiae*. Molecular and Cellular Biology. 17: 6223-6235.

Thoma, F. 1999. Light and dark in chromatin repair: repair of UV-induced DNA lesions by photolyase and nucleotide excision repair. The EMBO Journal. 18: 6585-6598.

Thuen. D. 2002. The effect of increased UV-B radiation on two aquatic organisms, *Carassius auratus* and *Daphnia magna*. Unpublished thesis, Department of Biology, University of Winnipeg.

Todo, T. 1999. Functional diversity of the DNA photolyase/blue light receptor family. Mutation Research, DNA Repair. 434: 89-97.

Todo, T., Ryo, H., Takemori, H., Toh, H., Nomura, T., and S. Kondo. 1994. High-level expression of the photorepair gene in Drosophila ovary and its evolutionary implications. Mutation Research, DNA Repair. 315: 213-228.

Uchida, N., Mitani, H., Todo, T., Ikenaga, M., and A. Shima. 1997. Photoreactivating enzyme for (6-4)photoproducts in cultured goldfish cells. Photochemistry and Photobiology. 65: 964-968.

Vetter, R. D., Kurtzman, A., and T. Mori. 1999. Diel cycles of DNA damage and repair in eggs and larvae of Northern Anchovy, *Engraulis mordax*, exposed to solar ultraviolet radiation. Photochemistry and Photobiology 69:27-33.

Vincent, W. F., and P. J. Neale. 2000. Mechanisms of UV damage to aquatic organisms *In* The effects of UV radiation in the marine environment. *Edited by* S. de Mora, S. Demers and M. Vernet. Cambridge University Press, London, pp. 149-176.

Whitehead, R. F., de Mora, S. J. and S. Demers. 2000. Enhanced UV radiation – a new problem for the marine environment. *In* The effects of UV radiation in the marine environment. *Edited by* S. de Mora, S. Demers and M. Vernet. Cambridge University Press, London, pp. 1-34.

Wiegand, M. D., Hataley, J. M., Kitchen, C. L., and L. G. Buchanan. 1989. Induction of developmental abnormalities in larval goldfish, *Carassius auratus* L., under cool incubation conditions. Journal of Fish Biology. 35: 85-95.

Yasuhira, S., Mitani, H., and A. Shima. 1991. Enhancement of photorepair of ultraviolet-damage by preillumination with florescent light in cultured fish cells. Photochemistry and Photobiology 53: 211-215.

Yasuhira, S., and A. Yasui. 1992. Visible light-inducible photolyase gene from the goldfish *Carassius auratus*. The Journal of Biological Chemistry 267: 25644-25647.

Yasui, A., Eker, A. P. M., Yasuhira, S., Yajima, H., Kobayashi, T., Takao, M., and A. Oikawa. 1994. A new class of DNA photolyases present in various organisms including aplacental mammals. The EMBO Journal 13: 6143-6151.

APPENDICES

A. Artificial Insemination Medium (AIM)

For a 2.0 L solution of AIM, combine 200 mL 200 mM Tris buffer, pH 9.19, and 64 mL of solution H (484 mM NaCl, 1.6 mM KCl, 9.8 mM $CaCl_2 \cdot 2H_20$) and 1736 mL of double distilled water.

B. Calf thymus DNA trials for testing protocol for detection of cyclobutane pyrimidine dimers using endonuclease sensitive site (ESS) assay. Adapted from Drouin (1997).

1. DNA was precipated by adding 3 M sodium acetate pH 7.0 for final concentration of 0.3 M and 2.5 volumes of 95% ethanol kept at –70°C and incubated at –70°C for 60 minutes.

2. Centrifuging for 20 minutes at 14000 rpm sedimented the DNA. Supernatant was removed and pellet was air dried until all the ethanol precipitated.

3. Pellet was resuspended in 20 μL double distilled water (ddH_2O) for a final concentration 0.5 μg/μL.

4. For electrophoresis, 6 μL 0.5 μg/μL DNA (3 μg) was added and gently mixed with 6 μL freshly prepared 100 mM NaOH: 4 mM EDTA solution and 8 μL denaturing loading buffer (1 mM NaOH, 50% v/v glycerol, 0.05% w/v bromocresol green).These solutions were incubated at room temperature for 20 minutes.

5. Samples were electrophoresed for 12 hours at 0.4 V/cm in 4°C. A 1% alkaline agarose gel (1% agarose, 50 mM NaCl, 1 mM EDTA) and alkaline running buffer (50 mM NaOH, 1 mM EDTA) were used to create denaturing conditions.

6. The gel was neutralized in 1 M Tris pH 8.0 for 30 minutes and stained in ethidium bromide (0.5 μg/mL) for 30 minutes.

C. Phenol-chloroform extraction of DNA from goldfish embryos.

1. Sufficient urea homogenizing buffer (100 μL – 200 μL) (7 M urea, 0.35 M NaCl, 0.01 M Tris pH 7.6, 1 mM EDTA, 2% SDS) (Ahmed and Setlow 1993) was added to double the volume of the embryos in the microfuge tubes.

2. On ice, the embryos were mashed using micropestles (Eppendorf) until the spinal cords are not visible.

3. The homogenate was incubate at 37°C for 60 minutes.

4. After incubation, the sample were spun in an Eppendorf microfuge at 14000 rpm at 4°C for 20 minutes.

5. The supernatant was transferred into a fresh microfuge tube and add an equal volume of phenol:chloroform (1:1) mixture. Phenol was buffered between pH 7 and 8 with Tris buffer.

6. The microfuge tubes were gently mixed by inversion and centrifuged for 1 minute at 14000 rpm to separate aqueous and organic phases.

7. The upper, aqueous phase was removed and transferred to a fresh microfuge tube.

8. An equal volume of chloroform was added and mixed by inversion.

9. To separate phases, the samples were centrifuged for 1 minute at 14000 rpm and the aqueous phase was transferred to a fresh tube.

10. Steps 8 and 9 would be repeated until minimal white debris remained at the interface between the organic and aqueous layers.

11. The upper phase was transferred into fresh tube and 0.7 volumes of isopropanol held at room temperature were added and mixed by inversion.

12. To pellet the DNA, the samples were centrifuged for 15 minutes at 14000 rpm.

13. The supernatant was removed and the pellet was washed with 500 μL 75% ethanol. The samples were centrifuged for 1 minute at 14000 rpm.

14. The supernatant was removed and the DNA air dried until all ethanol evaporated.

15. Once dry, the pellets were suspended in 50 μL sterile double distilled water. Dissolution often took overnight. The samples were stored at –20°C until required.

D. Goldfish DNA trials: Protocol for detection of cyclobutane pyrimidine dimers using endonuclease sensitive site (ESS) assay. Adapted from Drouin (1997).

1. After quantification, DNA was precipitated by adding 10 μL 3M sodium acetate pH 7.0, to a final concentration of 0.3 M, and 125 μL 95% ethanol stored at –70°C.

2. Samples were incubated at –70°C for 60 minutes and centrifuged for 20 minutes at 14000 rpm in 4°C. The supernatant was removed and the pellet air dried.

3. The pellets were suspended in a volume of digestion buffer (50 mM Tris-HCl pH 7.6, 1 mM EDTA, 50 mM NaCl, 1 mM β-mercaptoethanol) based on the amount of DNA determined from quantification. The final concentration of DNA was of 0.25 μg/μL.

4. 10 μg DNA (40-50 μL) are transferred into a new microfuge tube. The DNA is incubated for 2 hours at 37°C with 6 units of T4 endonuclease V (Interscience, Inc.) and 2 μL of RNase (500 μg/mL, Roche Applied Science) and incubate for 2 hours at 37°C.

5. After digestion, 3 M sodium acetate pH 7.0 for final concentration of 0.3 M and 2.5 volumes of 95% ethanol kept at –70°C were added. The DNA was precipitated by incubated at –70°C for 60 minutes.

6. DNA was sedimented by centrifuging for 20 minutes at 14000 rpm at 4°C. The supernatant was removed and the pellet was air dried.

7. Once dry, the pellet was resuspended in 20 μL of double distilled water for a final concentration 0.5 μg/μL.

8. For electrophoresis, 6 μL 0.5 μg/μL DNA (3 μg) was added and gently mixed with 6 μL freshly prepared 100 mM NaOH: 4 mM EDTA solution and 8 μL denaturing loading buffer (1 mM NaOH, 50% v/v glycerol, 0.05% w/v bromocresol green). The samples were incubated at room temperature for 20 minutes.

9. The samples were electrophoresed for 12 hours at 0.8 V/cm in 4°C using a 1% alkaline agarose gel (1% agarose, 50 mM NaCl, 1 mM EDTA) that had been soaking in alkaline running buffer (50 mM NaOH, 1 mM EDTA) for several hours prior to electrophoresis.

10. The gel was neutralized in 1 M Tris buffer (pH 8.0) for 30 minutes and stained in ethidium bromide (0.5 μg/mL) for 30 minutes with shaking.